JCB Article

# The yeast protein kinase Mps1p is required for assembly of the integral spindle pole body component Spc42p

**Andrea R. Castillo,[1] Janet B. Meehl,[1] Garry Morgan,[1] Amy Schutz-Geschwender,[2] and Mark Winey[1]**

[1]MCD Biology, UCB 347, University of Colorado, Boulder, CO 80309
[2]LI-COR Inc., Lincoln, NE 68504

*Saccharomyces cerevisiae MPS1* encodes an essential protein kinase that has roles in spindle pole body (SPB) duplication and the spindle checkpoint. Previously characterized *MPS1* mutants fail in both functions, leading to aberrant DNA segregation with lethal consequences. Here, we report the identification of a unique conditional allele, *mps1–8,* that is defective in SPB duplication but not the spindle checkpoint. The mutations in *mps1-8* are in the noncatalytic region of *MPS1*, and analysis of the mutant protein indicates that Mps1-8p has wild-type kinase activity in vitro. A screen for dosage suppressors of the *mps1-8* conditional growth phenotype identified the gene encoding the integral SPB component *SPC42*. Additional analysis revealed that *mps1-8* exhibits synthetic growth defects when combined with certain mutant alleles of *SPC42*. An epitope-tagged version of Mps1p (Mps1p-myc) localizes to SPBs and kinetochores by immunofluorescence microscopy and immuno-EM analysis. This is consistent with the physical interaction we detect between Mps1p and Spc42p by coimmunoprecipitation. Spc42p is a substrate for Mps1p phosphorylation in vitro, and Spc42p phosphorylation is dependent on Mps1p in vivo. Finally, Spc42p assembly is abnormal in a *mps1-1* mutant strain. We conclude that Mps1p regulates assembly of the integral SPB component Spc42p during SPB duplication.

## Introduction

In *Saccharomyces cerevisiae*, the spindle pole body (SPB)* serves as the centrosome equivalent organelle. SPBs are duplicated once each cell cycle and function to nucleate microtubules that will form the mitotic spindle. Proper SPB duplication is required to form a bipolar spindle, which in turn is essential for cells to accurately segregate their DNA. SPB morphology is distinct from the typical centrosome of animal cells, having a trilaminar disc-like structure instead of centrioles surrounded by pericentriolar material (Byers and Goetsch, 1974; Kochanski and Borisy, 1990). The SPB remains embedded in the nuclear envelope throughout the cell cycle, allowing it to simultaneously nucleate nuclear and cytoplasmic microtubules (Byers and Goetsch, 1974). Despite morphological differences between the SPB and centrosome, there are several conserved components (Adams and Kilmartin, 2000). These include proteins that form the γ-tubulin complex in *S. cerevisiae* (Spc98p, Spc97p, and Tub4p), the centrin homologue, Cdc31p, and the molecular spacer protein, Spc110p (Kendrin) (Byers, 1981; Kilmartin et al., 1993; Geissler et al., 1996; Spang et al., 1996; Knop et al., 1997; Middendorp et al., 1997; Flory et al., 2000). Although the γ-tubulin complex clearly serves to nucleate microtubules in both the SPB and the centrosome, the conserved function performed by Cdc31p and Spc110p is still unclear (Moritz et al., 1995; Zheng et al., 1995; Knop and Schiebel, 1997; Marshall and Wilson, 1997; Adams and Kilmartin, 2000).

The SPB duplication pathway has been described through EM analysis of wild-type cells and mutant cells that fail at different stages of SPB duplication (Byers and Goetsch, 1975; Adams and Kilmartin, 1999). Duplication of the SPB occurs in G1 of the cell cycle, beginning with the accumulation of SPB components (the satellite) onto the cytoplasmic face of the half-bridge, a modification of the nuclear envelope distal to the SPB (Byers and Goetsch, 1975). The amorphous satellite appears to develop into a larger ordered structure

Address correspondence to Mark Winey, MCD Biology/UCB 347, University of Colorado, Boulder, CO 80309-0347. Tel.: (303) 492-3409. Fax: (303) 492-7744. E-mail: mark.winey@colorado.edu

*Abbreviations used in this paper: GFP, green fluorescent protein; GST, glutathione *S*-transferase; SPB, spindle pole body.

A.R. Castillo's present address is Div. of Basic Sciences, Fred Hutchison Cancer Research Laboratory, 1100 Fairview Ave. N. A2-168, Seattle, WA 98109.

Key words: budding yeast; spindle pole body; *MPS1*; *SPC42*; protein kinase

called the duplication plaque (Adams and Kilmartin, 1999; O'Toole et al., 1999). Immuno-EM analysis of the satellite and duplication plaque show both structures are composed of the core SPB components, Spc29p, Spc94p/Nud1p, Spc42p, and Cnm67p (Adams and Kilmartin, 1999). Assembly of the new SPB is completed when the duplication plaque is inserted into the nuclear envelope and associates with additional SPB components that will make up the inner (nuclear) plaque layers (Adams and Kilmartin, 1999).

The terminal phenotype of various SPB duplication mutants has suggested when the gene products might be required in the process (Byers and Goetsch, 1975; Rose and Fink, 1987; Winey et al., 1991; Schutz et al., 1997; Schutz and Winey, 1998). For example, yeast containing a mutant *SPC42* gene fail in SPB duplication after satellite formation (Donaldson and Kilmartin, 1996). The *SPC42* gene product forms the electron-dense (two-dimensional crystalline) central layer of the SPB, and Spc42p is found in the duplication intermediates, the satellite, and duplication plaque (Donaldson and Kilmartin, 1996; Bullitt et al., 1997; Adams and Kilmartin, 1999; O'Toole et al., 1999). Unlike mutant alleles of *SPC42*, different mutant alleles of *MPS1*, which encodes a dual specificity protein kinase required for SPB duplication, fail at two distinct points in SPB duplication (Winey et al., 1991; Lauze et al., 1995; Schutz and Winey, 1998). This suggests that Mps1p is required for multiple events in SPB duplication.

Mps1p is unusual in that it has a role in the spindle checkpoint and in SPB duplication (Hardwick and Murray, 1995; Weiss and Winey, 1996). Kinetochores that are not attached to microtubules activate the spindle checkpoint (Wang and Burke, 1995; Pangilinan and Spencer, 1996). Failed SPB duplication also triggers this checkpoint, possibly because a monopolar spindle does not nucleate a sufficient number of microtubules to capture all of the kinetochores and cannot produce tension via bipolar spindle attachment (Winey and O'Toole, 2001). The conditional *MPS1* mutants isolated thus far are defective in both pathways; therefore, under restrictive conditions *MPS1* mutant cells proceed through mitosis with a monopolar spindle, aberrantly segregate their DNA, and rapidly lose viability (Winey et al., 1991; Schutz and Winey, 1998). Although the role of Mps1p in this checkpoint is not yet clearly defined, it requires kinase activity and is probably accomplished through phosphorylation of another checkpoint component, Mad1p (Hardwick et al., 1996).

Previously, we used a *mps1-1* strain in genetic screens to identify interactions that would enhance our understanding of the role of Mps1p in SPB duplication and the spindle checkpoint (Schutz et al., 1997; Jones et al., 1999). We identified genes involved in the spindle checkpoint, spindle function, and those involved in stabilizing the Mps1p kinase (Hofmann et al., 1998; Jones et al., 1999). However, we did not identify SPB components. Here, we characterize a novel conditional allele, *mps1-8*, that is specifically defective in SPB duplication and use this allele in a dosage suppressor screen. We identified *SPC42*, a gene that encodes an integral SPB component, as a dosage suppressor of the *mps1-8* conditional growth defect. We use genetic and biochemical techniques to investigate the interaction between Mps1p and Spc42p, taking advantage of an Spc42p in vivo assembly assay (Donaldson and Kilmartin, 1996) to show that Mps1p is required for Spc42p assembly.

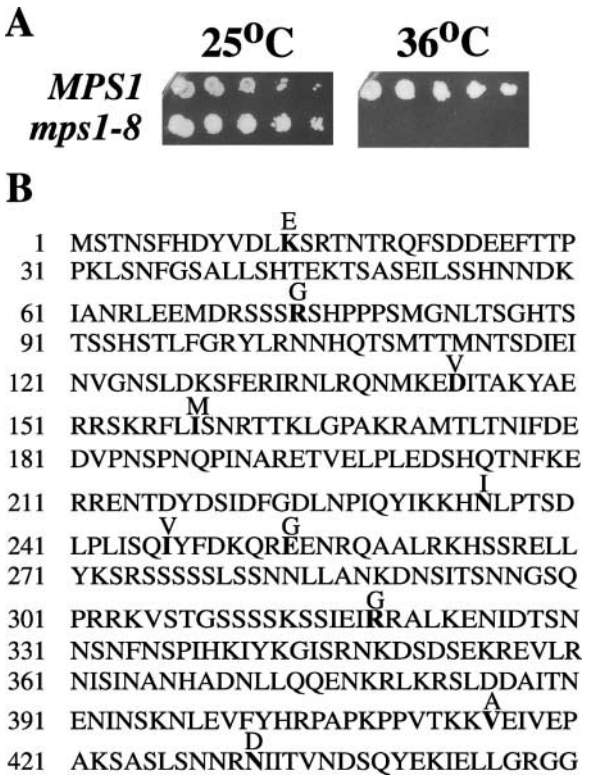


Figure 1. **A new *MPS1* allele, *mps1-8*, contains mutations in the noncatalytic region that result in conditional growth at 36°C.** (A) A wild-type (WX257-14c) and *mps1-8* (ACY54-9b) strain was grown to saturation at 25°C and plated in fivefold serial dilution on rich media. These plates were incubated at 25 or 36°C for 4 d. The *mps1-8* strains fail to grow at the restrictive temperature of 36°C. (B) Sequencing of the noncatalytic region (amino acids 1-450) of *mps1-8* revealed 10 point mutations that resulted in amino acid changes (K13E, R74G, D143V, I158M, N235I, I244V, E254G, R319G, V415A, N429D).

## Results

### A novel mps1 temperature-sensitive for growth allele

We have investigated further the essential role of *MPS1* by generating and characterizing a novel conditional *MPS1* mutation, defective only in SPB duplication. This *MPS1* allele was isolated from a library of mutagenized *MPS1* clones prepared by amplifying the noncatalytic ($NH_2$-terminal) region of *MPS1* using error-prone PCR. We targeted this region of *MPS1* for mutagenesis because (a) existing conditional *MPS1* alleles have mutations in the catalytic domain and are defective in both Mps1p functions and (b) deletion analysis showed the $NH_2$ terminus is required for function (unpublished data; Schutz and Winey, 1998). We used a strain that allowed us to screen simultaneously for different *MPS1*-associated phenotypes (*mps1Δ::KanMX cin8Δ::HIS3*, supported by counter-selectable plasmids) (see Materials and methods). Counter selection of the plasmid containing *CIN8* allowed us to identify *MPS1* alleles that might be defective in the spindle checkpoint function of *MPS1* (see Ma-

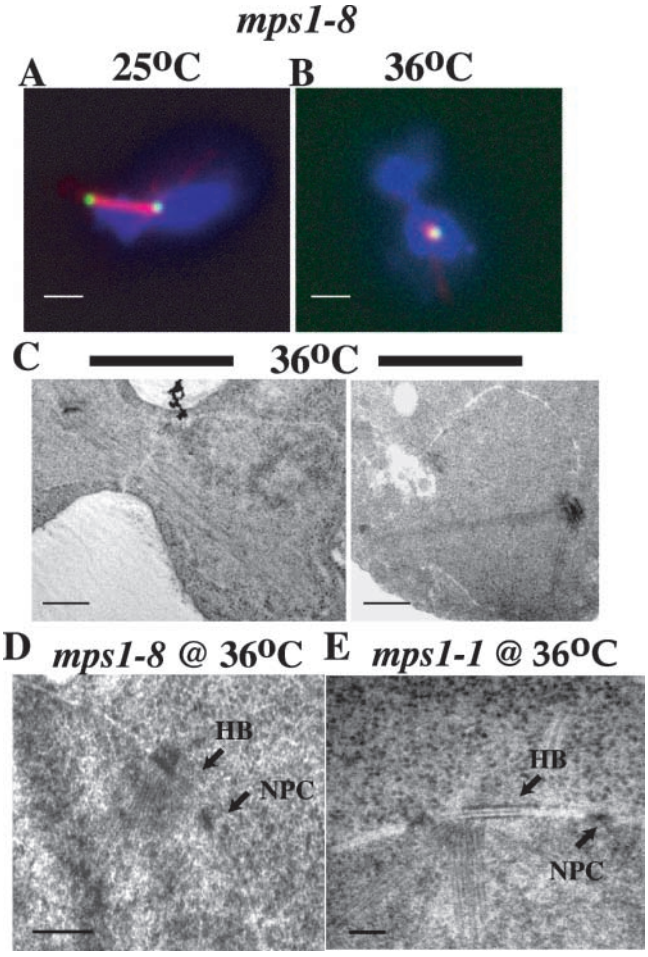


Figure 2. ***mps1-8* cells fail in SPB duplication when grown at their restrictive temperature (36°C).** (A and B) Immunofluorescence images of a *mps1-8* (ACY71-14b) strain grown at the permissive (A, 25°C) or restrictive (B, 36°C) temperature for 3 h after release from an α-factor–induced G1 arrest. These cells were fixed and stained with DAPI to visualize DNA (blue), an antibody against α-tubulin to visualize microtubules (red), and Spc42-GFP in this strain (ACY71-14b) identifies the SPBs (green). (A) In *mps1-8* cells grown at the permissive temperature (25°C), two foci of Spc42-GFP in the large budded cell indicates that the SPB has duplicated. In this image, a short spindle can be seen between the two SPBs. (B) At the restrictive temperature (36°C), only a single foci of GFP signal is observed in large budded cells (92%, $n = 42$), indicating SPB duplication has failed to occur. (C–E) Electron micrographs of asynchronously growing *mps1-8* (ACY66-4) and *mps1-1* (WX241-3b) diploids shifted to the restrictive temperature for 5 h. An unduplicated SPB was detected in serial sections of large budded *mps1-8* and *mps1-1* cells. Only one section is shown here. The unduplicated SPB of *mps1-8* cells (D; $n = 17$) is associated with half-bridge (HB, arrow) material but lacks the extended half-bridge typical of *mps1-1* mutants (E, HB, arrow). NPC, nuclear pore complex. Bars: (A and B) 2.0 μm; (C) 0.4 μm; (D) 0.2 μm; (E) 0.1 μm.

terials and methods) (Geiser et al., 1997). These alleles will be described elsewhere. Using temperature sensitivity as a screen for potential SPB duplication defects, we isolated *mps1-8* (Fig. 1 A) and showed it is a recessive mutation (unpublished data).

Sequencing revealed that *mps1-8* contained multiple mutations (Fig. 1 B); none of the 10 mutations that resulted in amino acid changes individually conferred conditional growth (unpublished data). It is likely that some combination of these mutations is responsible for the *mps1-8* phenotype, and all further analysis was performed using the original *mps1-8* allele.

## mps1-8 mutants fail in SPB duplication

We have established previously that the essential *MPS1* cellular function is in SPB duplication (Weiss and Winey, 1996). To test if the *mps1-8* conditional growth defect might reflect this role, we monitored SPB duplication in *mps1-8* cells using immunofluorescence microscopy and EM. Asynchronously growing *mps1-8* cells were arrested in G1 using the mating pheromone α-factor, released to the permissive (25°C) or restrictive (36°C) temperature for 3h, and processed for indirect immunofluorescence. The majority of *mps1-8* cells complete SPB (shown in green) duplication at 25°C as expected, but they fail to duplicate their SPB at 36°C (92%, $n = 42$; Fig. 2, A and B). Instead, these cells show a typical *S. cerevisiae* mitotic arrest state with large buds in which the single unduplicated SPB is associated with cellular DNA (blue) and a focus of microtubules (red) (Fig. 2 B). By immunofluorescence, the SPB duplication defect in the *mps1-8* strain is identical to the SPB defect observed in previously characterized conditional *MPS1* mutants (Schutz and Winey, 1998).

The morphology of the SPB in *mps1-8* cells grown at the restrictive temperature was further examined using EM (see Materials and methods). Serial sections of large budded cells were examined, and a single SPB was found in all cases, verifying that SPB duplication fails in *mps1-8* cells grown at the restrictive temperature. As in other *MPS1* mutants, the unduplicated SPB in *mps1-8* cells is associated with half-bridge material, but unlike them this structure is not elongated in *mps1-8* cells (Fig. 2, C–E) (Winey et al., 1991; Schutz and Winey, 1998). It is not yet clear if the subtle difference in the terminal SPB phenotype of the *mps1-8* mutant and other *MPS1* mutants indicates they are failing at different points in SPB duplication.

## mps1-8 mutants are competent to activate the spindle checkpoint

As mentioned, the previously characterized conditional *MPS1* mutants are defective in both SPB duplication and the spindle checkpoint (Winey et al., 1991; Weiss and Winey, 1996; Schutz and Winey, 1998). We show that the *mps1-8* mutant fails in SPB duplication at the restrictive temperature. To determine if *mps1-8* cells also fail in the spindle checkpoint, we compared the *mps1-8* strain with *mps1-1*, a strain known to be defective in activating the spindle checkpoint, and *mps2-1*, a strain able to activate the spindle checkpoint with a monopolar spindle (Hardwick et al., 1996; Weiss and Winey, 1996). Asynchronously growing cultures of *mps1-8*, *mps1-1*, and *mps2-1* cells were synchronized in G1 with α-factor, released at 25 or 36°C, and samples for flow cytometry and budding indices were taken after 2 and 3 h. At the restrictive temperature, *mps1-8* cells exhibit a mitotic arrest similar to that observed for *mps2-1* cells; the majority of the cells have a large budded cell morphology, a G2 DNA content (Fig. 3, A and B), and accumu-

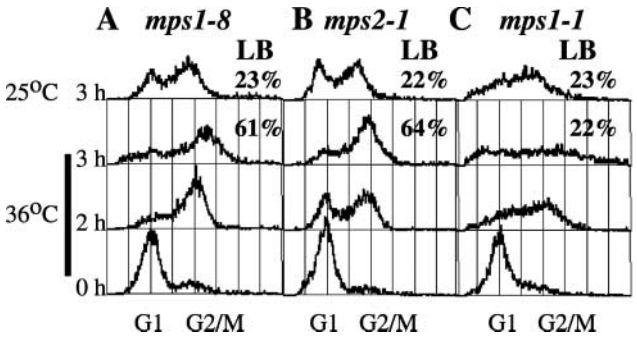


Figure 3. ***mps1-8* cells arrest in mitosis through activation of the spindle checkpoint.** Asynchronously growing *mps1-8* (ACY54-9b), *mps2-1* (SMY-1b), and *mps1-1* (WX241-10c) strains were arrested in G1 using α-factor and then released at both permissive (25°C) and restrictive (36°C) temperatures. Samples for flow cytometry were collected at $T = 0$ (G1 arrest), 2, and 3 h after release from the G1 arrest (only the 3-h time point shown for cells at 25°C). (A) The mitotic arrest observed in *mps1-8* cells at the restrictive temperature is seen as the accumulation of cells with a G2 DNA content and large budded (LB) cell morphology (61%). At the permissive temperature, *mps1-8* cells return to cycling asynchronously. (B) For comparison, *mps2-1* cells also arrest in mitosis after they fail in SPB duplication at the restrictive temperature. (C) A *mps1-1* strain serves as a negative control for a mutant that fails to arrest in mitosis after SPB duplication fails at the restrictive temperature. In these histograms, the x-axis is the relative DNA content determined by propidium iodide fluorescence, and the y-axis is the number of cells with the given DNA content (as described in Materials and methods). Peaks corresponding to normal haploid G1 and G2 DNA content are indicated on the x-axis. Each sample represents 5,000 cells.

late hyperphosphorylated forms of the spindle checkpoint protein Mad1p, a molecular marker for spindle checkpoint activation (unpublished data; Hardwick et al., 1996). In contrast, the *mps1-1* strain fails to arrest in mitosis when grown at the restrictive temperature and instead accumulates cells that appear aploid or aneuploid by flow cytometry (Fig. 3 C). We conclude that *mps1-8* is a novel mutant allele leading to defects in SPB duplication but maintaining a functional spindle checkpoint.

## Mps1-8p exhibits wild-type levels of kinase activity

We were interested in assessing the level of kinase activity associated with Mps1-8p. To determine this, we compared kinase activity in vitro at the *mps1-8* permissive (25°C) and restrictive (36°C) temperatures using protein generated from galactose-inducible glutathione *S*-transferase (GST) fusion constructs, containing GST alone, GST-MPS1, GST-mps1-1, GST-mps1-KD (kinase dead), and GST-mps1-8 (see Materials and methods). The relative specific activity associated with GST–mps1-8p is similar to that observed for the wild-type protein at either the *mps1-8* permissive or restrictive temperature (Fig. 4 A). GST–mps1-1p and GST–mps1-KD were used as controls for *MPS1* mutant proteins that have negligible catalytic activity at either assay temperature (Fig. 4 B) (Lauze et al., 1995; Schutz and Winey, 1998). By Western analysis, both GST-Mps1p and GST–Mps1-8p migrate as broad bands slower than the predicted molecular weight of 112 kD (Fig. 4 B) (Lauze et al., 1995; Schutz and Winey, 1998). The band shift observed was shown previously for

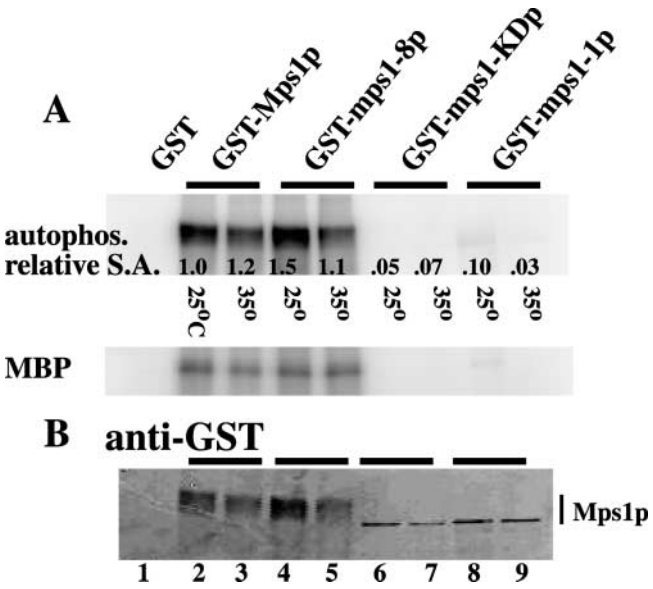


Figure 4. **Autophosphorylation by GST-tagged mps1-8p is similar to wild-type Mps1p.** Plasmids carrying the GST-tagged *MPS1* alleles, *mps1-8*, *mps1-1*, *mps1-KD* (kinase dead), and *MPS1* (and GST alone), were transformed into the wild-type W303 strain, and expression of the fusion proteins was induced as described in Materials and methods. The fusion proteins were isolated and used to do kinase assays in vitro at the *mps1-8* permissive (25°C) and restrictive (35°C) temperatures (as described in Materials and methods). (A) Proteins were resolved on an SDS-PAGE gel and transferred to nitrocellulose. Autophosphorylation by the GST-tagged proteins and their ability to phosphorylate an exogenous substrate, myelin basic protein (MBP), were quantitated on a phosphorimager (as described in Materials and methods). (B) The amount of GST-tagged protein in each lane was quantitated using a fluorescence-based imaging system (as described in Materials and methods). Relative specific activity (S.A.) of GST–mps1-8p at both 25°C (lane 4, 1.5) and 35°C (lane 5, 1.1) is similar to that observed for GST-Mps1p at either temperature (lane 2, 1.0, and lane 3, 1.2). For comparison, the kinase-dead version of Mps1p (GST-mps1-KDp) has undetectable levels of autophosphorylation at either assay temperature (lanes 6 and 7). As reported previously (Schutz and Winey, 1998), GST–mps1-1p has minimal kinase activity at temperatures permissive (lane 8, 25°C, 0.01) for *mps1-1* mutant strain growth and no kinase activity at temperatures restrictive (lane 9, 35°C, 0.03) for growth. Phosphorylation of MBP mirrors the autophosphorylation observed for the GST-tagged proteins in these kinase assays.

wild-type protein to be due to autophosphorylation (Fig. 4, A and B). The ability of GST–mps1-8p to phosphorylate an exogenous substrate, myelin basic protein, was also comparable to that observed for the wild-type protein (Fig. 4 B). Therefore, our in vitro results suggest that the SPB duplication defect associated with *mps1-8* is not due to a loss of kinase activity itself, but may reflect inappropriate localization or other regulation of Mps1p.

## A dosage suppressor of mps1-8

A dosage suppressor screen was performed in a *mps1-8* strain to identify genes whose products might interact with Mps1p during SPB duplication. We transformed a *mps1-8* strain with a 2-μ URA-based yeast genomic library and screened for transformants that were able to restore growth at 36°C (see Materials and methods). In addition to isolating two

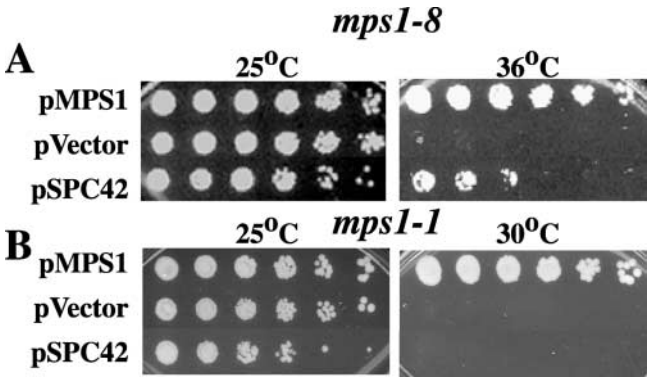


Figure 5. ***SPC42* is an allele-specific dosage suppressor of the *mps1-8* conditional growth defect.** *mps1-8* (BD8WX257–5c) (A) and *mps1-1* (B) strains (WX241-10c) were transformed with p2μ-URA-MPS1, p2μ-URA-SPC42, or vector alone. These transformants were grown to $OD_{600}$ = 3.0, plated in fivefold serial dilution on $URA^-$ media, and the plates grown at either permissive (25°C) or restrictive temperatures for *mps1-8* (A, 36°C) and *mps1-1* (B, 30°C). (A) Increased dosage of *SPC42* confers intermediate growth to the *mps1-8* strain at a temperature (36°C) normally restrictive for growth. (B) This suppression is not observed for the *mps1-1* strain containing p2μ-URA-SPC42. As expected, both strains containing p2μ-URA-MPS1 grow well at the restrictive temperature but fail to grow at the restrictive temperature when they contain the vector alone.

different *MPS1*-containing clones (multiple times), five unique clones were identified as suppressors of the *mps1-8* conditional growth defect. In one of these clones (S81), we identified *SPC42* as the ORF responsible for *mps1-8* suppression (Fig. 5 A). *SPC42* mutants exhibit defects in SPB duplication, and Spc42p is a phosphoprotein that localizes to the central plaque of the SPB and duplication intermediates in the satellite and duplication plaque (Donaldson and Kilmartin, 1996; Adams and Kilmartin, 1999). Increased dosage of *SPC42* only suppressed the *mps1-8* phenotype and not *mps1-1* (Fig. 5 B), *mps1-737*, *mps1-412*, *mps1-1237*, or *mps1-3796* (unpublished data). This suggests that the *mps1-8* defect is distinct from the previously characterized conditional *MPS1* mutants.

Two well-characterized *SPC42 ts* mutants, *spc42-10* and *spc42-11* (Donaldson and Kilmartin, 1996), exhibit a monopolar phenotype similar to *MPS1* mutants when grown at their restrictive temperatures. We generated the double mutant strains, *mps1-8 spc42-10* and *mps1-8 spc42-11* to look for additional genetic interactions between *SPC42* and *MPS1* (see Materials and methods). Both double mutant strains show enhanced growth defects when compared with either single mutant strain (unpublished data). The genetic interactions between *MPS1* and *SPC42* suggest that the gene products may interact in vivo.

## Mps1p localizes to the SPB and kinetochores

The genetic interaction of *MPS1* with a bona fide integral SPB component suggested that Mps1p might localize to SPBs, which we initially tested using immunofluorescence microscopy on whole cells. Asynchronously growing cells containing myc epitope-tagged *MPS1* at the *MPS1* locus (Mps1p-myc) and *SPC42* tagged with green fluorescent protein (GFP) (Spc42-GFP) were analyzed by immunofluorescense (see Materials and methods). We observe a strong signal of Mps1p-myc (red) that partially overlaps Spc42p-GFP (green), primarily in unbudded cells, and diffuse nuclear staining (Fig. 6 A). Similar localization was observed with a ProA-tagged Mps1 protein (Schutz et al., 1997; Steiner, 1998). This Mps1p signal is suggestive of SPB and/or kinetochore localization, since yeast kinetochores are adjacent to the SPB during G1 of the cell cycle (Wigge et al., 1998; Wigge and Kilmartin, 2001).

To better characterize Mps1p localization, we determined if Mps1p-myc colocalizes with the kinetochore protein Ndc10p using chromosome spread analysis. A strain containing Mps1p-myc and Ndc10p-HA was grown to midlog phase and samples were harvested for chromosome spread analysis. The diffuse nuclear Mps1p-myc signal we observed by whole cell immunofluorescence appears to overlap with signal from Ndc10p-HA (Fig. 6 B). We also observed Mps1p-myc colocalization with Spc42p-GFP using chromosome spread analysis (Fig. 6 B). In examining chromosome spreads where a single SPB was labeled by Spc42-GFP, and the criterion of ≥90% overlap of Mps1p-myc with Spc42-GFP was considered colocalization, we found that 43% of the spreads ($n$ = 54) exhibited colocalization of these proteins. As a control, we did the same analysis in spreads of strains expressing Spc42-GFP and Ndc10p-HA, and we found only 20% of these spreads showed ≥90% overlap of the two proteins ($n$ = 54), indicating that chromosome spreads can be used to resolve SPBs and kinetochores. Using this technique, Mps1p is found at both organelles.

Finally, we performed immuno-EM on asynchronously growing strains containing Mps1p-myc. Colloidal gold signal overlapping the SPB in the plane of the nuclear envelope suggests that Mps1p localizes to the Spc42p central plaque region (5 examples in 24 cells examined) (Fig. 6 C). Mps1p signal is also detected at the end of microtubules by immuno-EM as is seen for other kinetochore proteins (Wigge et al., 1998; Wigge and Kilmartin, 2001) (18 examples in 24 cells examined) (Fig. 6 D). This dual localization is consistent with a role for Mps1p in SPB duplication and the spindle checkpoint.

## Mps1p and Spc42p physically interact

The genetic interactions between *MPS1* and *SPC42* and their colocalization at the SPB prompted us to investigate their physical interaction in the cell. Extracts were prepared from cells containing (a) Mps1p-myc, (b) Ndc1p-myc, as a control for nonspecific interaction with the myc epitope, and (c) no tag. These proteins were immunoprecipitated with anti-myc antibody conjugated to agarose beads and resolved using SDS-PAGE. The presence of Mps1p-myc and Ndc1p-myc was detected using an anti-myc antibody (Fig. 7 B, lanes 5 and 6). Polyclonal anti-Spc42p antibody was used in a duplicate Western analysis and detected a band migrating at the expected molecular weight (46–51 kD) for Spc42p in the Mps1p immunoprecipitate but not the Ndc1p immunoprecipitate (Fig. 7 A, lanes 1 and 2). Indeed, this band migrates at approximately the same position as

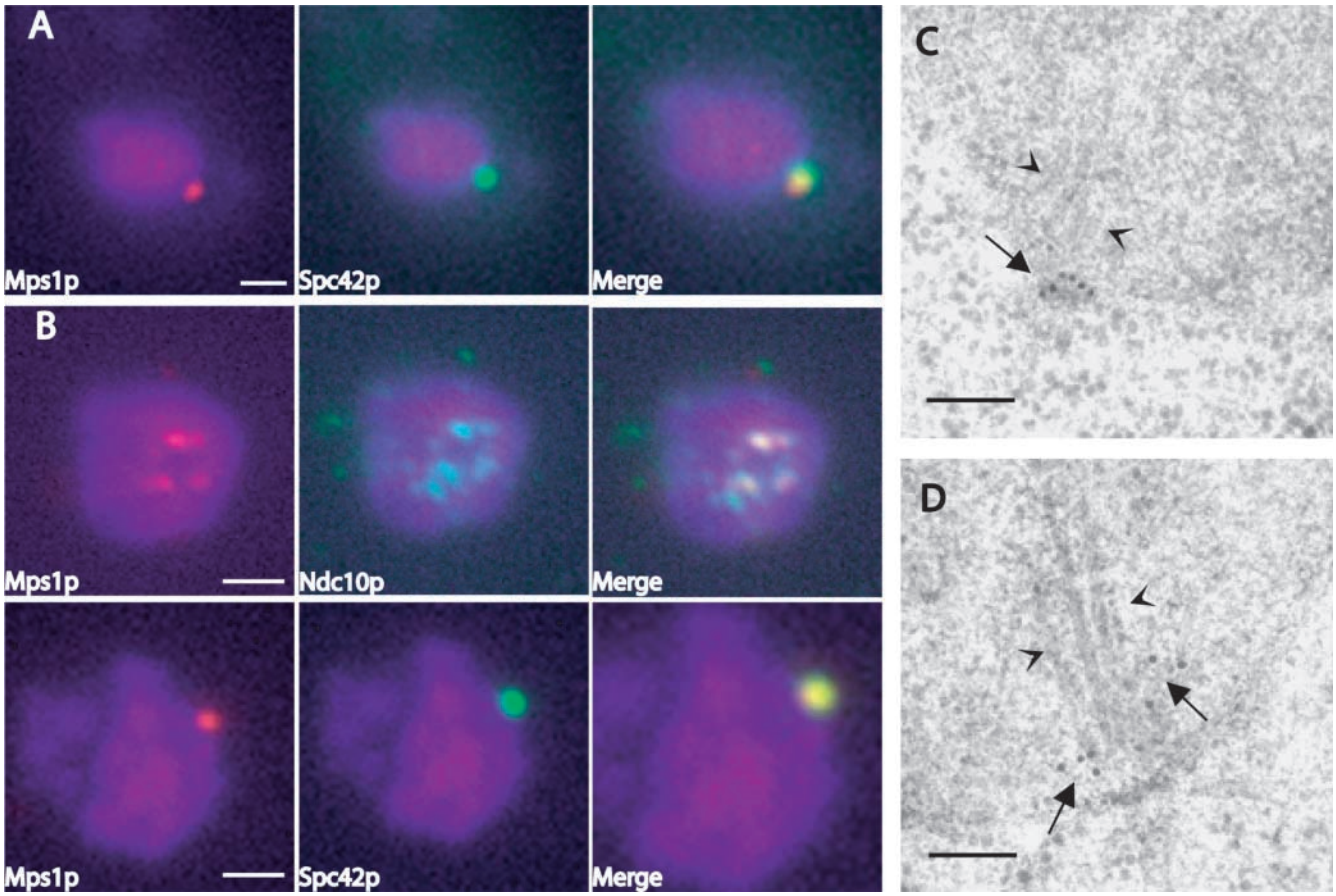


Figure 6. **Mps1p-myc localizes to the SPB and the kinetochores.** (A) Cells containing *MPS1-myc* and *SPC42-GFP* (JM7) were grown to mid-log phase, harvested, and then fixed and stained for indirect immunofluorescence. DAPI was used to visualize DNA (blue), an affinity purified anti-myc polyclonal antibody was used to identify Mps1p-myc (red), and a polyclonal anti-GFP antibody was used against Spc42-GFP (green). (A) Mps1p-myc signal is observed as faint dots coincident with DAPI staining and a more intense dot that colocalizes with Spc42-GFP signal. (B) Chromosome spreads prepared from a strain containing Mps1p-myc (red) and Ndc10p-HA (green) (JM16) or Mps1p-myc (red) and Spc42p-GFP (green) (JM43) show localization of Mps1p-myc to the kinetochores and SPB. (C and D) Immuno-EM of strains containing Mps1p-myc shows colloidal gold signal coincident with the central plaque of the SPB (C, arrows) and at the plus end of microtubules nucleated from the SPB (D, arrows). Arrowheads in C and D indicate microtubules. Bars: (A and B) 1.0 μm; (C and D) 0.1 μm.

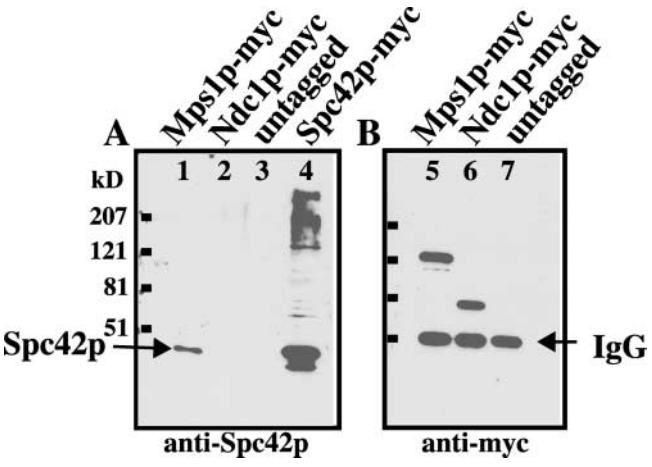


Figure 7. **Mps1p and Spc42p physically interact.** Clarified extracts (as described in Materials and methods) made from asynchronously growing cultures of a *MPS1-myc* strain (SBY650), a *NDC1-myc* strain (HC12–2b), and an untagged strain were incubated with anti-myc monoclonal antibody conjugated to agarose beads to immunoprecipitate the myc-tagged proteins. Immunoprecipitated protein samples were divided and resolved by SDS-PAGE to produce duplicate gels. One blot (A, lanes 1–4) was probed using polyclonal anti-Spc42p, and a second blot (B, lanes 5–7) was probed with an anti-myc antibody. Spc42p specifically coimmunoprecipitates with Mps1p-myc (lane 1), since Spc42p is not detected in either the Ndc1p-myc or untagged control lanes (lanes 2 and 3). A whole cell lysate from a strain overexpressing Spc42p-myc (ACY122-1c) was used to indicate where Spc42p would migrate. Lanes 5 and 6 show that the Mps1-myc and NDC1-myc proteins are present. Lane 7 contains an immunoprecipitate from the untagged strain and shows where the IgG band migrates (IgG band also seen in lanes 5 and 6).

Spc42p-myc, isolated from a strain overexpressing Spc42p-myc (Fig. 7 A, lane 4). Thus, Mps1p and Spc42p both localize at the SPB and physically interact with each other.

### Spc42p is a substrate in vitro for Mps1p, and Spc42p phosphorylation is dependent on Mps1p

Spc42p is a phosphoprotein whose phosphorylation state varies throughout the cell cycle (Donaldson and Kilmartin, 1996). To determine if Spc42p is a substrate for Mps1p, we used Mps1p-myc and recombinant Spc42p in a kinase assay

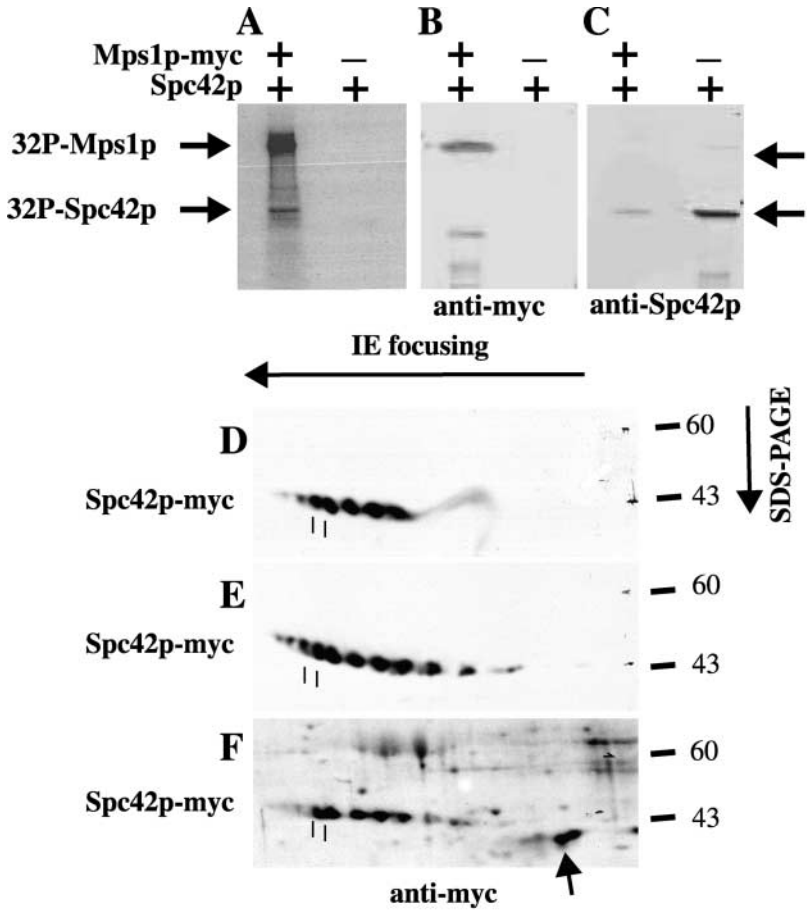


Figure 8. **Spc42p is a substrate in vitro for Mps1p, and Spc42p phosphorylation is dependent on Mps1p in vivo.** A kinase assay was performed in vitro using Mps1p-myc immunoprecipitated (as described in Materials and methods) from an asynchronously growing strain (SBY650). Recombinant Spc42p purified from baculovirus-infected insect cells (a gift from Danni Vinh and Trisha Davis, University of Washington, Seattle, WA) was used as a substrate in this assay. Kinase reactions were resolved using SDS-PAGE, and the gel was transferred to nitrocellulose. A fluorescence-based imaging system allowed us to use the same nitrocellulose blot to assess $^{32}P$ incorporation and for Western analysis (as described in Materials and methods) to detect Mps1p-myc and Spc42p. (A) Signal corresponding to autophosphorylation of Mps1p-myc and phosphorylation of Spc42p was observed in the reaction where both Mps1p-myc and Spc42p were present (arrows). No signal was observed when Mps1p-myc was not included in the reaction. (B) Western blotting with an anti-myc antibody shows that Mps1p-myc is present in lane 1, and anti-Spc42p antibody shows that Spc42p is present in both reactions (C). (D–F) Two-dimensional gel analysis (as described in Materials and methods) of whole cell extracts prepared from *MPS1 GAL-SPC42-myc* (ACY122-1c) and *mps1-1 GAL-SPC42-myc* (ACY123-10a) strains, that were released from an α-factor arrest into inducing media at the *mps1-1* nonpermissive temperature (D), indicates that Spc42p phosphorylation is dependent on Mps1p. Only 6 of the 11 spots corresponding to Spc42p-myc in the *MPS1* strain (E) were present in the *mps1-1* strain (D). When extract from *MPS1 GAL-SPC42-myc* was treated with calf alkaline phosphatase before two-dimensional gel analysis, seven spots were detected (F). Five of these spots correspond to those detected in the *mps1-1* strain (D and F). The other two (F, arrow) are in a new position, relative to those identified in the *MPS1* strain, migrating faster and more basic as might be expected for less phosphorylated forms of Spc42p-myc. The two dashed lines under spots (D–F) are for orientation.

in vitro. A band corresponding to Spc42p was detected by autoradiography (Fig. 8, A, lane 1) and the presence of this band was dependent on the addition of Mps1p-myc (Fig. 8 A, lane 2). Additionally, we observed autophosphorylation of Mps1p-myc (Fig. 8 A), which has been reported previously (Lauze et al., 1995).

We subsequently assessed whether phosphorylation of Spc42p was dependent on Mps1p function in vivo. We were unable to detect differences in the phosphorylation state of Spc42p-myc isolated from *MPS1* and *mps1-1* strains using one-dimensional SDS-PAGE (unpublished data). However, differences in Spc42p phosphorylation were revealed using two-dimensional gel electrophoresis (Fig. 8, D–F). For this assay, *MPS1* and *mps1-1* strains containing *SPC42-myc* under the control of the galactose promoter were arrested in G1 using α-factor and then released into inducing media at the *mps1-1* restrictive temperature for 2 h. Extracts were prepared from these samples and resolved by two-dimensional gel electrophoresis and blotted to PVDF membranes. 11 spots corresponding to Spc42p-myc were identified on the two-dimensional blot prepared using the *MPS1* extract (Fig. 8 E). Only six of these spots were detected on the blot prepared using the *mps1-1* extract (Fig. 8 D). We believe that the absence of these forms of Spc42p-myc in the *mps1-1* strain is due to the inability of Mps1-1p to phosphorylate Spc42p-myc at the *mps1-1* restrictive temperature. Indeed,

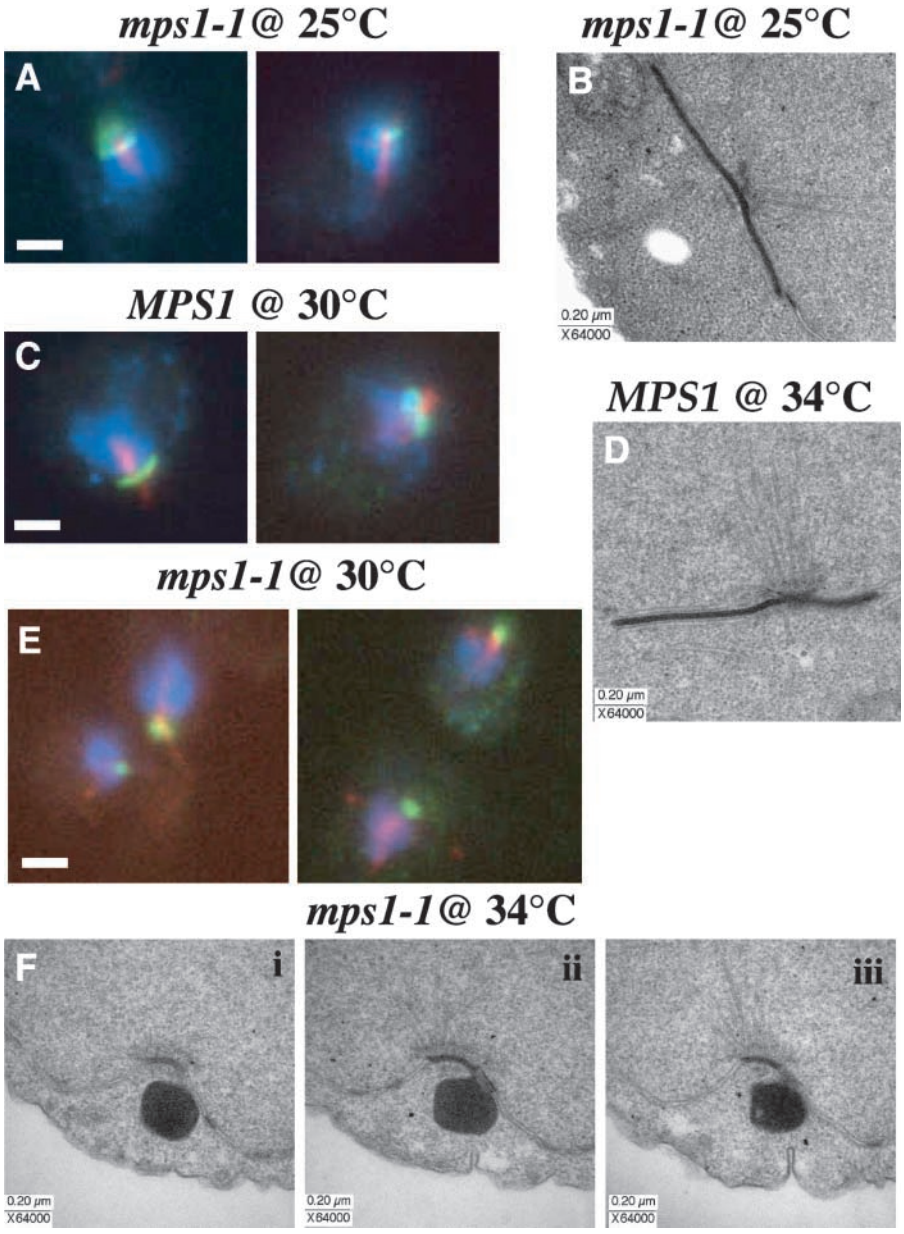


Figure 9. **Spc42p assembly is compromised in the *mps1-1* mutant background.** Asynchronously growing *MPS1 GAL-SPC42-myc* (ACY122-1c) and *mps1-1 GAL-SPC42-myc* (ACY123-10a) strains were arrested in G1 using α-factor and then released at both 25 and 30°C into galactose-containing media to induce overexpression of *SPC42-myc* (under control of *GAL1,10* promoter). Samples were collected for indirect immunofluorescence 3 h after release into inducing media (A, C, and E); DNA is stained with DAPI (blue), and antibodies were used to detect α-tubulin (red) and the myc epitope of Spc42-myc (green). A similar experiment was performed to generate samples for EM (B, D, and F). The only modification was that the strains were released from α-factor into inducing media at 25 and 34°C. Samples were high pressure frozen and processed for EM (as described in Materials and methods). Formation of the organized "super plaque" composed of Spc42-myc protein is observed in *mps1-1* (two cells are shown) and *MPS1* (unpublished data) cells grown at 25°C (A) and in *MPS1* cells grown at 30°C (two cells shown) (C). (E) An apparently smaller less organized Spc42-myc protein structure forms in *mps1-1* cells grown at the *mps1-1* restrictive (30°C; four cells shown) temperature. (F) Serial EM sections (i, ii, iii) reveal that this Spc42-myc structure forms at the half-bridge of the existing SPB and lacks the symmetry reported previously for the "super plaque" (Donaldson and Kilmartin, 1996). The "super plaque" observed in *mps1-1* cells grown at the *mps1-1* permissive (25°C) temperature and in *MPS1* cells grown at 34°C (B and D) have a morphology similar to that reported previously for the "super plaque" (Donaldson and Kilmartin, 1996). Bars: (A, C, and D) 1.0 μm.

when we treated extract from the *MSP1* strain with calf alkaline phosphatase before two-dimensional analysis, the same five spots of Spc42p-myc were absent (Fig. 8 F). The phosphatase-treated sample is missing an additional form of Spc42p-myc detected in the untreated *MPS1* extract and shows accumulation of two new forms of Spc42p-myc (Fig. 8 F). Loss of this additional form of Spc42p in the phosphatase-treated sample suggests that another kinase may contribute to Spc42p phosphorylation. The new forms of Spc42p migrate faster and in a more basic position than forms present in the untreated *MPS1* sample, suggesting that they are less phosphorylated or unphosphorylated forms of Spc42p (Fig. 8 F, arrow). Interestingly, we do not detect these new forms of Spc42p-myc in the *mps1-1* strain. Failure of the phosphatase treatment to produce a single form of Spc42p-myc could be due to incomplete dephosphorylation of Spc42p-myc or to additional posttranslational modification on Spc42p. Phosphorylation of Spc42p by Mps1p in vitro and dependence on Mps1p in vivo suggests that Mps1p may regulate Spc42p during SPB duplication.

### Misassembly of Spc42p in MPS1 mutant cells

Overexpression of Spc42p-myc from an inducible promoter results in the lateral expansion of the central layer of the SPB so that organized layers of Spc42p extend from the SPB in all directions and appear to rest on the nuclear envelope (Donaldson and Kilmartin, 1996; Bullitt et al., 1997; O'Toole et al., 1999). This "super plaque" structure appears by EM to be organized into a two-dimensional crystalline lattice identical to what is observed for Spc42p in the central plaque of a normal SPB (Bullitt et al., 1997). Spc42p isolated from both of these structures is phosphorylated; however, it is not yet clear what role phosphorylation of Spc42p might play in their assembly (Donaldson and Kilmartin, 1996). Here, we analyze formation of the "super plaque" upon *SPC42* overexpression in *MPS1* mutants. The assem-

bly assay was performed in *MPS1* and *mps1-1* strains at permissive (25°C) and restrictive temperatures (30 and 34°C) for *mps1-1*. These strains also contained a myc epitope-tagged version of *SPC42* under the control of a galactose-inducible promoter *(GAL-SPC42-myc*).

Proper formation of the "super plaque" was first analyzed using immunofluorescence. The *MPS1 GAL-SPC42-myc* and *mps1-1 GAL-SPC42-myc* strains were grown in noninducing media (no galactose), arrested in G1 using α-factor, and then released into galactose-containing media at both 25 and 30°C for 3 h to induce expression of *GAL-SPC42-myc*. At the permissive temperature, the *mps1-1* (Fig. 9 A) and *MPS1* (unpublished data) strains form Spc42p-myc–dependent dome-like structures (super plaque in green) that are associated with DNA (blue) and microtubule (red) signal. The "super plaque" formed in the wild-type strain at 30°C is identical to what we observe for this strain at 25°C (Fig. 9 C). By contrast, in the *mps1-1* strain at 30°C we observe a decrease in Spc42p-myc signal at the SPB, and it has a much less organized appearance (Fig. 9 E). To characterize these structures at higher resolution, we analyzed them using EM (see Materials and methods).

Overexpression of *SPC42-myc* in the wild-type and *mps1-1* strain at the permissive temperature results in the formation of the organized dome-shaped "super plaque." These structures extend laterally from the central plaque of the SPB but appear to be constrained vertically to ~23 nm as reported previously for the "super plaque" (Fig. 9, B and D) (Bullitt et al., 1997). In contrast, it is clear that Spc42p-myc signal in the *mps1-1* strain at the restrictive temperature is an unorganized mass of electron-dense material associated with the half-bridge of the unduplicated SPB (Fig. 9 F). Based on the EM section width (80 nm), we estimate that the structure shown is ~300 nm × 480 nm × 250 nm (Fig. 9 F). This structure is similar to one formed when *spc42-S:A*, a mutant allele in which 34 serines have been mutated to alanines, is overexpressed at similar levels (Adams and Kilmartin, 1999). This data suggests that Mps1p function, via phosphorylation of Spc42p, is required for the proper assembly of the central layer of the new SPB during SPB duplication.

## Discussion

We have identified a physical interaction between the integral SPB component Spc42p and Mps1p, a regulator of Spc42p assembly during SPB duplication. We show that Mps1p is capable of phosphorylating Spc42p in vitro and its phosphorylation is dependent on Mps1p in vivo. Additionally, in vivo assembly of Spc42p is compromised in a *MPS1* mutant (*mps1-1*). Mps1-1p has essentially no kinase activity in vitro; therefore, we believe that phosphorylation of Spc42p by Mps1p is important for the assembly of Spc42p into the SPB. We investigated interactions between Mps1p and Spc42p based on our isolation of *SPC42* as a dosage suppressor of a unique *MPS1* mutant, *mps1-8*. This conditional mutant was identified in a screen designed to separate the role of *MPS1* in SPB duplication from its role in the spindle checkpoint. Using immunofluorescence and EM, we show that *mps1-8* mutants fail to duplicate their SPBs at restrictive temperatures. Unlike previously characterized conditional *MPS1* mutants, *mps1-8* cells are competent to arrest in mitosis through activation of the spindle checkpoint after SPB duplication fails (Schutz and Winey, 1998). Therefore, *mps1-8* is an important genetic tool for our further investigation of the role of Mps1p in SPB duplication.

### mps1-8 is a unique allele

Mutations in the noncatalytic region of *MPS1* generated a conditional mutant, *mps1-8*, that is specifically defective in SPB duplication. We targeted the noncatalytic region of *MPS1* for mutagenesis, believing that this region might confer spatial or temporal regulation of Mps1p for each of its roles. In fact, our screen also identified a *MPS1* allele that appears to be specifically defective in the spindle checkpoint (to be described elsewhere). In this paper, we show that the molecular defect associated with *mps1-8* is likely distinct from our previously characterized conditional *MPS1* mutants. Mutations are in the noncatalytic region of *mps1-8* and do not affect kinase activity of the mutant protein. By contrast, other conditional *MPS1* mutants previously characterized in our lab have mutations in the catalytic region of the gene that affect kinase activity measured in vitro (Schutz and Winey, 1998).

Consistent with the notion that the *mps1-8* defect is distinct from other conditional *MPS1* mutants, *mps1-8* shows unique genetic interactions. We show that *mps1-8* but not the other conditional *MPS1* mutants is suppressed by an increased dosage of the Mps1p in vitro substrate, Spc42p. By contrast, several of the *MPS1* kinase mutants but not *mps1-8* are suppressed by an increased dosage of the molecular chaperone *CDC37* (Schutz et al., 1997). Although it is likely that *CDC37* suppresses through stabilization of the jeopardized Mps1p kinase, it is less clear how *SPC42* suppression occurs. We propose that suppression by *SPC42* may be through stabilizing an interaction between Spc42p and Mps1-8p. Alternatively, extra Spc42p may help localize Mps1-8p to the SPB or another site of action required for SPB duplication. Future localization studies and coimmunoprecipitation experiments using Mps1-8p should address these questions.

### Multiple requirements for Mps1p in SPB duplication

This and previous analyses suggest that Mps1p is required for multiple steps in SPB duplication (Winey et al., 1991; Schutz and Winey, 1998). Here, we show that *mps1-8* mutant cells fail very early in SPB duplication when grown at their restrictive temperature. By EM analysis, the unduplicated SPB in *mps1-8* cells is similar to those observed in *cdc31* and *kar1* mutants (Baum et al., 1986; Rose et al., 1986). The unduplicated SPB of *mps1-8* does not have an extended half-bridge that is characteristic of several other *MPS1* mutants (Winey et al., 1991; Schutz and Winey, 1998). This suggests that there are two distinct requirements for Mps1p early in SPB duplication. Alternatively, the functions defined by *mps1-8* and the other conditional *MPS1* mutants are not mutually exclusive; proper spatial regulation of Mps1p and Mps1p kinase activity may both be required for its early SPB function. Presumably, the *MPS1* kinase domain mutants proceed further in SPB duplication because the mutant proteins localize properly or make appropriate

physical interactions, though they are unable to function; the extended half-bridge might be a result of failed attempts to initiate SPB duplication.

*MPS1* also functions late in SPB duplication. *mps1-737* mutants assemble the central and outer layers of the new SPB but like *ndc1*, *mps2*, and *bbp1* mutants fail to insert this structure into the nuclear envelope (Winey et al., 1991, 1993; Schramm et al., 2000). Whereas these proteins may function to insert the duplication plaque into the nuclear envelope by providing an opening in the nuclear envelope, it is unclear how Mps1p is involved in this process (Chial et al., 1998; Munoz-Centeno et al., 1999; Schramm et al., 2000). One possibility is that Mps1p facilitates insertion of the duplication plaque into the nuclear envelope by controlling assembly of the inner plaque, a structure not formed in the *mps1-737* mutant. Two of the six proteins that make up the inner plaque, Spc110p and Spc98p, are substrates for Mps1p in vitro, and their phosphorylation is dependent on Mps1p in vivo (Pereira et al., 1998; Friedman et al., 2001). The *mps1-737* mutant phenotype might reflect a disrupted interaction with Spc110p and Spc98p or the inability of Mps1-737p to phosphorylate Spc110p and Spc98p. The multiple *MPS1* mutant phenotypes are consistent with Mps1p, playing a regulatory role in SPB duplication.

### Mps1p is required for Spc42p assembly

We investigated the role of Mps1p as a regulator of SPB assembly using a Spc42p in vivo assembly assay. Overexpression of Spc42p at very high levels causes the central plaque of the SPB (normal site of Spc42p localization) to extend laterally and form a structure we call the "super plaque." We believe that Mps1p might function in assembly of the central plaque during SPB duplication based on *MPS1* mutant phenotypes and because Mps1p physically interacts with and colocalizes with Spc42p in vivo and regulates Spc42p phosphorylation. When Spc42p was overexpressed in a *mps1-1* mutant at restrictive temperatures, we observed a defect in assembly of the "super plaque." This structure is not vertically confined to the two-dimensional crystalline lattice typically seen in *MPS1* cells overexpressing *SPC42* (Donaldson and Kilmartin, 1996; Adams and Kilmartin, 1999). A similar structure is detected when *spc42-S:A*, a mutant allele in which 34 serines have been mutated to alanines, is overexpressed at similar levels (Adams and Kilmartin, 1999). Since *spc42-S:A* is functional at endogenous levels, we believe this common overexpression phenotype reveals the importance of phosphorylation for proper plaque assembly that apparently results in different phenotypes when some phosphorylation is lost (the *spc42-S:A* allele with threonines intact) versus when most phosphorylation is lost (mutations in the kinase) (Adams and Kilmartin, 1999). In fact, Mps1-1p is severely compromised for kinase activity, and the *mps1-1* mutant accumulates fewer phosphorylated forms of Spc42p. We suspect that the phenotype we observe results from the inability of Mps1-1p to properly phosphorylate Spc42p. Failure of Mps1-1p to phosphorylate Spc42p during SPB duplication should then prevent assembly of the central plaque of the new SPB; consistent with this prediction, *mps1-1* cells do not show accumulation of satellite material at the half-bridge (Winey et al., 1991).

Is Mps1p function required for assembly of other satellite components? We suspect that Mps1p is required indirectly for assembly of Nud1p, Cnm67p, and Spc29p; Mps1p is required for assembly of Spc42p that may serve as a scaffold upon which the other satellite components assemble. This is supported by the unique suppression of *mps1-8* by increased dosage of *SPC42*. *NUD1*, *CNM67*, and *SPC29* were not identified in our screen as dosage suppressors of *mps1-8* or earlier as dosage suppressors of the *mps1-1* (Schutz et al., 1997). We tested *SPC29* directly and verified that increased dosage of *SPC29* does not suppress *mps1-8* (unpublished data). This does not preclude that the function of Mps1p is required for assembly of the other satellite components; the development of assembly assays for Nud1p, Cnm67p, and Spc29p will allow for investigation of the requirement for Mps1p in assembling these components. Regardless of other requirements for Mps1p in SPB duplication, the specific interaction established between Mps1p and Spc42p in this analysis indicates that their association is essential for assembly of the central plaque, an event that may be critical for launching SPB duplication.

## Materials and methods

### Yeast and *Escherichia coli* culture and genetic techniques

Yeast strains used in this study are listed in Table I and are derived from S288c and W303 backgrounds. Yeast and *E. coli* genetic techniques were as described by Ausubel et al. (1997). Yeast synchronization and 5-fluoroorotic acid screening were done as in Jones et al. (1999). Galactose (GAL) induction was done as in Hardwick et al. (1996).

### Protein techniques and kinase assays

GST fusion proteins were induced and isolated and kinase assays were performed as in Schutz and Winey (1998). Mps1p-13Xmyc (Ndc1p-3Xmyc isolated similarly, HC12–2b) was isolated from an asynchronously growing strain (SBY650) using techniques similar to those described in Schutz and Winey (1998). Mps1p-13Xmyc and recombinant Spc42p expressed in baculovirus-infected insect cells (a gift from Danni Vinh, Trisha Davis Lab, University of Washington, WA) were used in kinase assays as described in Lauze et al. (1995). Samples for all kinase assays were resolved on 15% Anderson SDS-PAGE gels (Anderson et al., 1973). Gels were subjected to electrophoretic transfer onto nitrocellulose membrane (Schleicher and Schuell Inc.) and membranes were used to expose a phosphorimager screen and for Western analysis to quantitate protein levels. $^{32}$P incorporation was quantitated using a Storm 860 phosphorImager with the ImageQuaNT analysis package (Molecular Dynamics). For Western analysis, nitrocellulose membranes were blocked using Odyssey blocker. Detection was performed using secondary antibodies labeled with the near-infrared fluorescent dyes IRDye800 and Cy5.5, and blots were scanned with an Odyssey Infrared Imager (Odyssey reagents, instruments, and software from LI-COR Biosciences). GST-Mps1 proteins were detected with goat antiglutathione primary antibody (1:1,000; Amersham Pharmacia Biotech) and an anti–goat antibody labeled with the IRDye800 fluorophore (1:10,000). Mps1p-13Xmyc was detected using an anti-myc primary antibody (1:1,000; Santa Cruz Biotechnology, Inc.) and an anti–mouse antibody labeled with IRDye800 (1:10,000). Spc42p was detected using a polyclonal anti-Spc42p primary antibody (a gift from John Kilmartin, Medical Research Council Laboratory of Molecular Biology, London, UK) and an anti–rabbit antibody labeled with Cy5.5 (1:10,000). Protein was visualized and quantitated with the Odyssey Imaging System.

We determined relative specific activity for each fusion protein by using the Storm860 phosphorImager and ImageQuaNT analysis package to measure $^{32}$P incorporation and by using the Odyssey Infrared Imager and analysis software to measure protein amounts. The number representing $^{32}$P incorporation was divided by the number representing protein amount to yield relative specific activity.

In the coimmunoprecipitate experiment, the immunoprecipitated material was resolved on an 8.5% laemmli SDS-PAGE gel (Ausubel et al., 1997). Gels were subjected to electrophoretic transfer onto a polyvinylidene difluoride membrane (Millipore). Polyvinylidene difluoride mem-

Table I. **Yeast strain list**

| Strain | Genotype | Source |
|---|---|---|
| SBY650 | *MATa,MPS1-13Xmyc::KanMX,ade2-1,bar1-1,can1-100* | S. Biggins[a] |
| LPY5 | *MATa,ade2-1,can1-100,his3-11,leu2-3,112,trp1-1,ura3-1* | L. Pillus[b] |
| HC12-2b | *MATa,NDC1-3Xmyc,ura3-52,trp1Δ1,his3Δ200, his4-539,ade2* | H.J. Chial[c] |
| WX257-14c | *MATa,ura3-52,his3Δ200,leu2-3,112,trp1Δ1* | Jones et al., 1999 |
| ACY17-16a | *MATa,mps1Δ::KanMX,cin8Δ::HIS3,trp1Δ1* (pURA-MPS1, pLEU-CIN8-cyh$^s$) | This study |
| WX257-8b | *MATα,ura3-52,his3Δ 200,leu2-3,112,trp1Δ1* | This study |
| ACY47-2a | *MATa,mps1ΔkanMX,ura3-52,his3Δ200,leu2-3,112,trp1Δ1* pRS314-MPS1 | This study |
| DB8WX257-5c | *MATa,mps1Δ::HIS3,ura3-52,trp1Δ1* pRS314-mps1-8 | Lauze et al. 1995 |
| ACY71-14b | *MATa,mps1Δ::KanMX,URA3::mps1-8,spc42Δ::LEU2,(TRP::SPC42-GFP)3X, leu2-3,112 his3Δ200,ade2-101,can1-100/GALpsi+,ssd1-d2* | This study |
| ACY66-4 | *MATa/MATα,mps1Δ::KanMX/mps1Δ::KanMX,URA3::mps1-8/URA3::mps1-8,his3Δ200/his3Δ200,leu2-3,112/leu2-3,112,trp1Δ1/trp1Δ1* | This study |
| WX241-3b | *MATa,mps1-1,ura3-52,his3Δ200,leu2-d* | This study |
| WX241-17a | *MATα,mps1-1,ura3-52,his3Δ200,trp1Δ1* | Schutz et al., 1997 |
| SMY7-1b | *MATa,mps2-1,his3Δ200,trp1Δ1,ura3-52,leu2-3,112* | S. McBratney[d] |
| WX241-20c | *MATa,mps1-1,ura3-52,his3Δ200* | Jones et al., 1999 |
| ACY54-9b | *MATa,mps1Δ::KanMX,URA3::mps1-8,his3Δ 200,leu2-3,112,trp1Δ1* | This study |
| WX241-10c | *MATa,mps1-1,ura3-52,his3Δ200* | Winey et al., 1991 |
| ACY139 | *MATα,spc42Δ::LEU2,ura3-52,trp1Δ1,his3Δ200,leu2-3,112* pRS202-SPC42 and pRS313-spc42-10 | This study |
| ACY140 | *MATα,ura3-52,trp1Δ1,his3Δ200,leu2-3,112* pRS202-SPC42 and pRS313-spc42-10 | This study |
| ACY141 | *MATa,mps1Δ::KanMX::mps1-8-TRP1,ura3-52,trp1Δ1,his3Δ200,leu2-3,112* pRS202-SPC42 and pRS313-spc42-10 | This study |
| ACY142 | *MATa,mps1Δ::KanMX::mps1-8-TRP1,spc42Δ::LEU2,ura3-52,trp1Δ1,his3Δ200,leu2-3,112* pRS202-SPC42 and pRS313-spc42-10 | This study |
| JM7 | *MATa,MPS1-13Xmyc-KanMX, spc42Δ::LEU2,TRP::SPC42-GFP(3X)* | This study |
| ACY123-10a | *MATa ,mps1-1,TRP::GAL-SPC42-3Xmyc,ura3-1,his3-11,leu2-3* | This study |
| ACY122-1c | *MATa,TRP::GAL-SPC42-3Xmyc,ura3-1,his3-11,leu2-3* | This study |
| JM16 | *MATa/MATα, MPS1-13Xmyc:KAN/MPS1,NDC10/NDC10:HA3:URA3:,leu- trp- his-* | This study |
| JM43 | *MATα,NDC10:HA3:URA3,spc42Δ:LEU2,TRP1:SPC42-GFP(3X),his-* | This study |

[a]Fred Hutchinson Cancer Research Center, Seattle, WA.
[b]University of California at San Diego, La Jolla, CA.
[c]University of Colorado.
[d]University of Colorado.

branes were blocked as in Chial et al. (1998). Mps1p-13Xmyc and Ndc1p-3Xmyc were detected using an anti-myc primary antibody (1:1,000; Santa Cruz Biotechnology, Inc.) and a sheep anti–mouse antibody conjugated to HRP (1:10,000; Sigma-Aldrich). Spc42p was detected using the anti-Spc42p polyclonal primary antibody (a gift from John Kilmartin, Medical Research Council Laboratory of Molecular Biology, London, UK) and a donkey anti–rabbit antibody conjugated to HRP (1:10,000; Sigma-Aldrich).

Alkaline phosphatase treatment of samples and two-dimensional gel electrophoresis were performed by Kendrick Labs, Inc. as described by Donaldson and Kilmartin (1996) and O'Farrell (1975), respectively. Isoelectric focusing was performed in glass tubes using 2% pH 4–8 ampholines (BDH ampholines Gallard Schlesinger) for 9,600 V/h. The tube gel was sealed to the top of a stacking gel on top of a 10% acrylamide slab gel. Samples were treated with 10 U of calf intestinal alkaline phosphatase (New England Biolabs, Inc.) at 30°C for 30 min.

## Cytological techniques

Flow cytometric analysis of cells was performed as described using the DNA stain propidium iodide (Sigma-Aldrich) (Hutter and Eipel, 1979). Samples were analyzed on a Becton Dickinson FACScan® flow cytometer using CELL QUEST software (Becton Dickinson).

Indirect immunofluorescence was performed as described in Chial et al. (1998), and chromosome spreads were performed as in Biggins et al. (1999). Tubulin was visualized using rat anti–α-tubulin primary antibody, YOL1/34 (1:150; Accurate Chemical), and anti–rat antibody conjugated to Texas red (1:400; Scientific). An affinity purified primary polyclonal anti-myc antibody (1:1,000; a gift from the Don W. Cleveland lab, University of California, San Diego, La Jolla, CA) and a donkey anti–rabbit Cy3-conjugated antibody (1:1,000; Scientific) were used to detect Mps1p-myc. In some experiments, a mouse anti-GFP primary antibody (1:40; a gift from the Pat O'Farrell lab, University of California, San Francisco, CA) and an anti–mouse FITC-conjugated antibody (1:800; Scientific) were used to detect Spc42-GFP. A monoclonal mouse anti-myc primary antibody (1:450) (9E10; Santa Cruz Biotechnology, Inc.) and anti–mouse FITC-conjugated antibody (1:800) (Jackson ImmunoResearch Laboratories) were used to detect Spc42p-myc. In chromosome spreads, a mouse anti-HA primary antibody (1:500) was used with an anti–mouse FITC-conjugated antibody (1:800). Fluorescent microscopy was performed using a Leica DMRXA/RF4/V automated microscope with a Cooke SensiCam digital camera and Slidebook software (Intelligent Imaging Innovations).

## EM

Cells for EM were prepared for thin sectioning by high pressure freezing and freeze substitution (Winey et al., 1995) or by chemical fixation (Byers and Goetsch, 1975). Serial thin sections were viewed on a Philips CM10 electron microscope (Philips Electronic Instruments), and images were captured on film or with a Gatan digital camera and viewed with the Digital Micrograph Software package (Gatan Inc.). Immuno-EM was performed using high pressure frozen and freeze-substituted cells as described by Giddings et al. (2001). Myc-tagged Mps1p was detected with polyclonal anti-myc antibody described earlier and 10 nM colloidal gold-conjugated secondary antibodies.

## Isolation of new MPS1 allele

Primers MPS1AC3 and MPS1AC4 were used to amplify the $NH_2$-terminus of *MPS1* (~2.2kb) under mutagenic PCR conditions: dATP = 0.1 mM, $MnCl_2$ = 0.5 mM, and $MgCl_2$ = 1.5 mM. 25, 20-μl PCR reactions were pooled, cut with EcoRI and BamHI, and ligated to EcoRI- and BamHI-digested pRS314-MPS1 to replace the wild-type $NH_2$ terminus. This ligation was used to transform *E. coli*, and transformants (805) were collected, grown for 2 h in Luria broth at 37°C, and prepared for DNA to make the *MPS1* mutagenized library.

We screened the *MPS1* mutagenized library in a strain (ACY17-16A) (Table I), *mps1Δ::KanMX cin8Δ::HIS3* pRS316-pac8-1, pLEU2-CIN8-cyh$^s$-CEN. pRS316-pac8-1 (*pac8-1* is an allele of *MPS1*) was maintained because *MPS1* is essential, and pLEU-CIN8-cyh$^s$-CEN was maintained be-

cause of the lethal interaction between *pac8-1* and *cin8Δ::HIS3* (Geiser et al., 1997). *mps1Δ::KanMX cin8Δ::HIS3* pRS316-pac8-1 plus pLEU-CIN8-cyh$^s$-CEN was transformed with the CEN-TR–based *MPS1* mutagenized library. 56% (17,920) of the TRP$^+$ transformants replica plated to 5-fluoroorotic acid were viable. These *mps1* alleles were tested for conditional growth at 36°C, benomyl (10 μg/ml; DuPont) sensitivity, and cycloheximide (5 μg/ml; Sigma-Aldrich) sensitivity. We isolated *mps1-8* as a conditional mutation (benomyl$^R$ and cycloheximide$^R$). We sequenced the mutagenized region of *mps1-8* using primers MPS1AC2, MPS1X, MPS1Y, and MPS1Z. Sequencing was done by the MCD Biology departmental sequencing facility (ABI automated sequencer).

The *mps1-8* allele was integrated at either the *URA3* or the *LEU2* locus. pRS306–mps1-8 was linearized with NcoI to direct integration at the *URA3* gene, and pRS305–mps1-8 was linearized with HpaI to direct integration at the *LEU2* gene. Proper integration at the *URA3* and *LEU2* loci was verified by PCR, using a primer internal to *MPS1* (MPS1AC7), and one within the *URA3* gene (ACURA3) or the *LEU2* (ACLEU2B).

### Dosage suppressor screen

We transformed a *mps1-8* strain with a 2-μ URA-based yeast genomic library (Connelly and Hieter, 1996) and screened 40,000 URA$^+$ transformants for growth at 36°C. 86 transformants grew at 36°C. We determined that 60 transformants exhibited plasmid-dependent growth at 36°C and isolated clones as done in Schutz et al. (1997). 22 clones conferred growth to *mps1-8* at 36°C upon retransformation. We used restriction digests to determine the number of unique, non*MPS1*, clones. Seven clones (S14, S36, S45, S47, S79, S81, S89) with unique genomic inserts and two different clones each containing *MPS1* were isolated multiple times. ORFs contained in these clones were identified as described in Jones et al. (1999). S81 contained three ORFs from chromosome XI, *YKL044W, PHD1*, and *SPC42*. *SPC42* was subcloned into pRS202, and we transformed the *mps1-8* strain with this clone and found that it conferred growth to *mps1-8* at 36°C. The other clones identified in this screen will be reported elsewhere.

We thank John Kilmartin for *SPC42* strains and antibody, Sue Biggins for the myc epitope-tagged *MPS1* strain and for her support, the Pat O'Farrell lab for anti-GFP antibody, Danni Vinh and Trisha Davis for Spc42p, the Don Cleveland laboratory for affinity purified anti-myc antibody, and Li-Cor Inc. for reagents and technical assistance. We are grateful to Corine Lau, Susan McBratney, Michele Jones, and Sue Jaspersen for critical reading of this article, Tom Giddings for advice on EM, and all Winey lab members for helpful discussions. A.R. Castillo was supported by an Individual National Research Service Award (National Institutes of Health grant GM19566 to A.R. Castillo). This work was also supported by the National Institute of Health (GM51312 to M. Winey).

Submitted: 7 November 2001
Revised: 19 December 2001
Accepted: 19 December 2001

## References

Adams, I.R., and J.V. Kilmartin. 1999. Localization of core spindle pole body (SPB) components during SPB duplication in *Saccharomyces cerevisiae. J. Cell Biol.* 145:809–823.

Adams, I.R., and J.V. Kilmartin. 2000. Spindle pole body duplication: a model for centrosome duplication? *Trends Cell Biol.* 10:329–335.

Anderson, C.W., P.R. Baum, and R.F. Gesteland. 1973. Processing of adenovirus-2 induced proteins. *J. Virol.* 12:241–252.

Ausubel, F.M., R. Brent, R.E. Kingston, D.D. Moore, J.G. Seidman, J.A. Smoth, and K. Struhl. 1997. Current protocols in molecular biology. John Wiley & Sons, Inc., New York. 50338 pp.

Baum, P., C. Furlong, and B. Byers. 1986. Yeast gene required for spindle pole body duplication: homology of its product with Ca2+-binding proteins. *Proc. Natl. Acad. Sci. USA.* 83:5512–5516.

Biggins, S., F.F. Severin, N. Bhalla, I. Sassoon, A.A. Hyman, and A.W. Murray. 1999. The conserved protein kinase Ipl1 regulates microtubule binding to kinetochores in budding yeast. *Genes Dev.* 13:532–544.

Bullitt, E., M. Rout, J. Kilmartin, and C. Akey. 1997. The yeast spindle pole body is assembled around a central crystal of Spc42p. *Cell.* 89:1077–1086.

Byers, B. 1981. Multiple roles of the spindle pole bodies in the life cycle of *Saccharomyces cerevisiae*. *Molecular Genetics of Yeast.* 16:119–133.

Byers, B., and L. Goetsch. 1974. Duplication of spindle plaques and integration of the yeast cell cycle. *Cold Spring Harb. Symp. Quant. Biol.* 38:123–131.

Byers, B., and L. Goetsch. 1975. Behavior of spindles and spindle plaques in the cell cycle and conjugation of S*accharomyces cerevisiae*. *J. Bacterial.* 124:511–523.

Chial, H.J., M.P. Rout, T.H. Giddings, and M. Winey. 1998. *Saccharomyces cerevisiae* Ndc1p is a shared component of nuclear pore complexes and spindle pole bodies. *J. Cell Biol.* 143:1789–1800.

Connelly, C., and P. Hieter. 1996. Budding yeast *SKP1* encodes an evolutionarily conserved kinetochore protein required for cell cycle progression. *Cell.* 86: 275–285.

Donaldson, A., and J. Kilmartin. 1996. Spc42p: a phosphorylated component of the *Saccharomyces cerevisiae* spindle pole body (SPB) with an essential function during SPB duplication. *J. Cell Biol.* 132:887–901.

Flory, M.R., M.J. Moser, R.J. Monnat, Jr., and T.N. Davis. 2000. Identification of a human centrosomal calmodulin-binding protein that shares homology with pericentrin. *Proc. Natl. Acad. Sci. USA.* 97:5919–5923.

Friedman, D.B., J.W. Kern, B.J. Huneycutt, D.B.N. Vinh, D.K. Crawford, E. Steiner, D. Scheilts, J. Yates, III, K.A. Resing, N.G. Ahn, et al. 2001. Mps1p phosphorylates the spindle pole component Spc110p in the N-terminal domain. *J. Biol. Chem.* 276:17958–17967.

Geiser, J., E. Schott, T. Kingsbury, N. Cole, L. Totis, G. Bhattacharyya, L. He, and A. Hoyt. 1997. *Saccharomyces cerevisiae* genes required in the absence of the *CIN8*-encoded spindle motor act in functionally diverse mitotic pathways. *Mol. Biol. Cell.* 8:1035–1050.

Geissler, S., G. Pereira, A. Spang, M. Knop, S. Soues, J. Kilmartin, and E. Schiebel. 1996. The spindle pole body component Spc98p interacts with the gamma-tubulin-like Tub4p of *Saccharomyces cerevisiae* at the sites of microtubule attachment. *EMBO J.* 15:3899–3911.

Giddings, T.H., Jr., E.T. O'Toole, M. Morphew, D.N. Mastronarde, J.R. McIntosh, and W. Winey. 2001. Using rapid freeze and freeze-substitution for preparation of yeast cells for electron microscopy and three-dimensional analysis. *Methods Cell Biol.* 67:27–42.

Hardwick, K., and A. Murray. 1995. Mad1p, a phosphoprotein component of the spindle assembly checkpoint in budding yeast. *J. Cell Biol.* 131:709–720.

Hardwick, K., E. Weiss, F.C. Luca, M. Winey, and A. Murray. 1996. Activation of the budding yeast spindle assembly checkpoint without mitotic spindle disruption. *Science.* 273:953–956.

Hofmann, C., I.M. Cheeseman, B.L. Goode, K.L. Mcdonald, G. Barnes, and D.G. Drubin. 1998. *Saccharomyces cerevisiae* Duo1p and Dam1p, novel proteins involved in mitotic spindle function. *J. Cell Biol.* 143:1029–1040.

Hutter, K.J., and H.E. Eipel. 1979. Microbial determination by flow cytometry. *J. Gen. Microbiol.* 113:369–375.

Jones, M.H., J.B. Bachant, A.R. Castillo, T.H. Giddings, Jr., and M. Winey. 1999. Yeast Dam1p is required to maintain spindle integrity during mitosis and interacts with the Mps1p kinase. *Mol. Biol. Cell.* 10:2377–2391.

Kilmartin, J., S. Dyos, D. Kershaw, and J. Finch. 1993. A spacer protein in the *Saccharomyces cerevisiae* spindle pole body whose transcript is cell cycle–regulated. *J. Cell Biol.* 123:1175–1184.

Knop, M., and E. Schiebel. 1997. Spc98p and Spc97p of the yeast γ-tubulin complex mediate binding to the spindle pole body via their interaction with Spc110p. *EMBO J.* 16:6985–6995.

Knop, M., G. Pereira, S. Geissler, K. Grein, and E. Schiebel. 1997. The spindle pole body component Spc97p interacts with the gamma-tubulin of *Saccharomyces cerevisiae* and functions in microtubule organization and spindle pole body duplication. *EMBO J.* 16:1550–1564.

Kochanski, R., and G. Borisy. 1990. Mode of centriole duplication and distribution. *J. Cell Biol.* 110:1599–1605.

Lauze, E., B. Stoelscker, F.C. Luca, E. Weiss, A. Schutz, and M. Winey. 1995. Yeast spindle pole duplication gene *MPS1* encodes an essential dual specificity protein kinase. *EMBO J.* 14:1655–1663.

Marshall, I., and K. Wilson. 1997. Nuclear envelop assembly after mitosis. *Trends Cell Biol.* 997:69–74.

Middendorp, S., A. Paoletti, E. Schiebel, and M. Bornens. 1997. Identification of a new mammalian centrin gene, more closely related to *Saccharomyces cerevisiae CDC31* gene. *Proc. Natl. Acad. Sci USA.* 94:9141–9146.

Moritz, M., M. Braufeld, J. Sedat, B. Alberts, and D. Agard. 1995. Microtubule nucleation by γ-tubulin-containing rings in the centrosome. *Nature.* 378: 638–640.

Munoz-Centeno, M.C., S. McBratney, A. Monterrosa, B. Byers, C. Mann, and M. Winey. 1999. *Saccharomyces cerevisiae MPS2* encodes a membrane protein localized at the spindle pole body and the nuclear envelope. *Mol. Biol. Cell.* 10:2393–2406.

O'Farrell, P.H. 1975. High resolution two-dimensional electrophoresis of proteins.

*J. Biol. Chem*. 250:4007–4021.

O'Toole, E., M. Winey, and J.R. McIntosh. 1999. High-voltage electron tomography of spindle pole bodies and early mitotic spindles in the yeast *Saccharomyces cerevisiae. Mol. Biol. Cell.* 10:2017–2031.

Pangilinan, F., and F. Spencer. 1996. Abnormal kinetochore structure activates the spindle assembly checkpoint in budding yeast. *Mol. Biol. Cell.* 7:1195–1208.

Pereira, G., M. Knop, and E. Schiebel. 1998. Spc98p directs the yeast gamma-tubulin complex into the nucleus and is subject to cell cycle-dependent phosphorylation on the nuclear side of the spindle pole body. *Mol. Biol. Cell.* 9:775–793.

Rose, M., and G. Fink. 1987. *KAR1*, a gene required for function of both intranuclear and extranuclear microtubules in yeast. *Cell.* 48:1047–1060.

Rose, M., B. Price, and G. Fink. 1986. *Saccharomyces cerevisiae* nuclear fusion requires prior activation by α factor. *Mol. Cell. Biol.* 6:3490–3497.

Schramm, C., S. Elliott, A. Shevchenko, and E. Schiebel. 2000. The Bbp1p-Mps2p complex connects the SPB to the nuclear envelope and is essential for SPB duplication. *EMBO J.* 19:421–433.

Schutz, A.R., and M. Winey. 1998. New alleles of the yeast *MPS1* gene reveal multiple requirements in spindle pole body duplication. *Mol. Biol. Cell.* 9:759–774.

Schutz, A.R., T.H. Giddings, E. Steiner, and M. Winey. 1997. The yeast *CDC37* gene interacts with *MPS1* and is required for proper execution of spindle pole body duplication. *J. Cell Biol.* 136:969–982.

Spang, A., S. Geissler, K. Grein, and E. Schiebel. 1996. γ-Tubulin–like Tub4p of *Saccharomyces cerevisiae* is associated with the spindle pole body substructures that organize microtubules and is required for mitotic spindle formation. *J. Cell Biol.* 134:429–441.

Steiner, E. 1998. Characterization of the *S. cerevisiae* Mps1 protein kinase. *In* Molecular, Cellular, and Developmental Biology. Ph.D. Thesis. University of Colorado, Boulder, CO. 143 pp.

Wang, Y., and D. Burke. 1995. Checkpoint genes required to delay cell division in response to nocodazole respond to impaired kinetochore function in the yeast *Saccharomyces cerevisiae. Mol. Cell. Biol.* 15:6838–6844.

Weiss, E., and M. Winey. 1996. The *Saccharomyces cerevisiae* spindle pole body duplication gene *MPS1* is part of a mitotic checkpoint. *J. Cell Biol.* 132:111–123.

Wigge, P.A., and J.V. Kilmartin. 2001. The Ndc80p complex from *Saccharomyces cerevisiae* contains conserved centromere components and has a function in chromosome segregation. *J. Cell Biol.* 152:349–360.

Wigge, P.A., O.N. Jensen, S. Holmes, S. Soues, M. Mann, and J.V. Kilmartin. 1998. Analysis of the *Saccharomyces* spindle pole by matrix-assisted laser desorption/ionization (MALDI) mass spectrometry. *J. Cell Biol.* 141:967–977.

Winey, M., and E.T. O'Toole. 2001. The spindle cycle in budding yeast. *Nat. Cell Biol.* 3:E23–E27.

Winey, M., L. Goetsch, P. Baum, and B. Byers. 1991. *MPS1* and *MPS2*: novel yeast genes defining distinct steps of spindle pole body duplication. *J. Cell Biol.* 114:745–754.

Winey, M., A. Hoyt, C. Chan, L. Goetsch, D. Botstein, and B. Byers. 1993. *NDC1*: a nuclear periphery component required for yeast spindle pole body duplication. *J. Cell Biol.* 122:743–751.

Winey, M., C. Mamay, E. O'Toole, D. Mastronarde, T. Giddings, K. McDonald, and R. McIntosh. 1995. Three dimensional ultrastructural analysis of the *Saccharomyces cerevisiae* mitotic spindle. *J. Cell Biol.* 129:1601–1615.

Zheng, Y., M. Wong, B. Alberts, and T. Mitchison. 1995. Nucleation of microtubule assembly by a γ-tubulin-containing ring complex. *Nature.* 378:578–583.